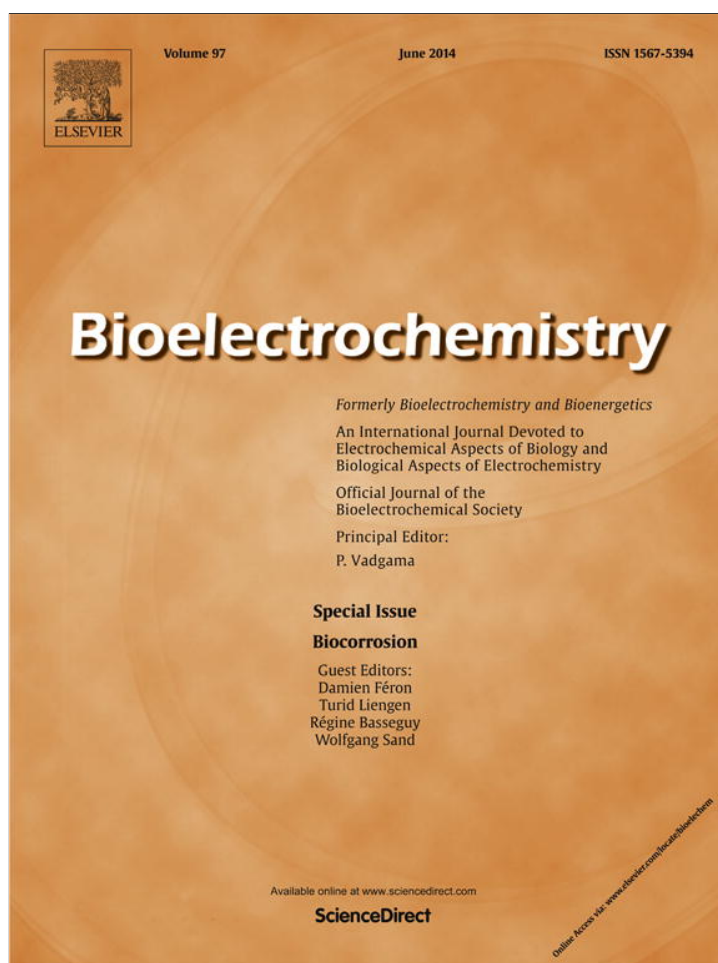


Provided for non-commercial research and education use.
Not for reproduction, distribution or commercial use.



This article appeared in a journal published by Elsevier. The attached copy is furnished to the author for internal non-commercial research and education use, including for instruction at the authors institution and sharing with colleagues.

Other uses, including reproduction and distribution, or selling or licensing copies, or posting to personal, institutional or third party websites are prohibited.

In most cases authors are permitted to post their version of the article (e.g. in Word or Tex form) to their personal website or institutional repository. Authors requiring further information regarding Elsevier's archiving and manuscript policies are encouraged to visit:

<http://www.elsevier.com/authorsrights>



Contents lists available at ScienceDirect

Bioelectrochemistry

journal homepage: www.elsevier.com/locate/bioelechem

Corrosion behaviour and biocorrosion of galvanized steel water distribution systems



F. Delaunois, F. Tosar, V. Vitry*

Metallurgy Lab, UMONS, 20 place du Parc, 7000 Mons, Belgium

ARTICLE INFO

Article history:

Received 11 December 2012

Received in revised form 15 January 2014

Accepted 15 January 2014

Available online 21 January 2014

Keywords:

Biocorrosion

Galvanized steel

Electrochemical impedance spectroscopy

Optical microscopy

ABSTRACT

Galvanized steel tubes are a popular mean for water distribution systems but suffer from corrosion despite their zinc or zinc alloy coatings.

First, the quality of hot-dip galvanized (HDG) coatings was studied. Their microstructure, defects, and common types of corrosion were observed. It was shown that many manufactured tubes do not reach European standard (NBN EN 10240), which is the cause of several corrosion problems. The average thickness of zinc layer was found at 41 μm against 55 μm prescribed by the European standard.

However, lack of quality, together with the usual corrosion types known for HDG steel tubes was not sufficient to explain the high corrosion rate (reaching 20 μm per year versus 10 $\mu\text{m}/\text{y}$ for common corrosion types).

Electrochemical tests were also performed to understand the corrosion behaviours occurring in galvanized steel tubes. Results have shown that the limiting step was oxygen diffusion, favouring the growth of anaerobic bacteria in steel tubes.

EDS analysis was carried out on corroded coatings and has shown the presence of sulphur inside deposits, suggesting the likely bacterial activity.

Therefore biocorrosion effects have been investigated. Actually sulphate reducing bacteria (SRB) can reduce sulphate contained in water to hydrogen sulphide (H_2S), causing the formation of metal sulphides. Although microbial corrosion is well-known in sea water, it is less investigated in supply water. Thus, an experimental water main was kept in operation for 6 months. SRB were detected by BART tests in the test water main.

© 2014 Elsevier B.V. All rights reserved.

1. Introduction

Metals used for water distribution system (cast iron, steel or copper) corrode due to their thermodynamic instability.

To avoid corrosion, steel pipes are covered by a protective layer of zinc or zinc alloy using Hot-Dip Galvanizing (HDG) [1,2]. This process consists in the immersion of steels parts in a molten zinc bath to obtain a coating thickness between 20 and 85 μm depending on quality specifications (NBN EN 10240). The structure of the zinc coating can be predicted by the Fe–Zn diagram. The various phases consist of several layers as shown in Fig. 1 [1–6].

The coating thickness is influenced by various factors, the main being chemical composition of the steel substrate. Actually, solute additions in some substrates, such as silicon and phosphorus, affect the growth rate of the various zinc layers during galvanization, resulting in a thick and brittle coating [1] with a too thick zeta phase (Sandelin effect) [4,5,7]. Bath and annealing temperatures have also major effects on the kinetics of the reactions [1,2].

The zinc coating protects steel against corrosion by the two following effects: a barrier effect due to the continuity of the coating that separates the steel from the corrosive environment and a galvanic protection because zinc acts as a sacrificial anode to protect the underlying steel [1,2]. Usually, a thickness of 55 μm (defined by European standard NBN EN 10240 as 396 g/m^2 , obtained by a gravimetric method) is advised for good protection of steel against generalized corrosion in fresh water [8]. However, a coating in which the zeta phase is absent or too thick and presents a columnar morphology [2,4–6] does not protect steel from generalized corrosion. To be efficient, the outer eta layer must represent at least 45% of the thickness of the whole coating [7].

Corrosion can also be accelerated either by high levels of chloride and sulphate in the water, by elevation of the temperature or by the pH of the water [1,3,5,6,8,9].

Various types of corrosion can be found in sanitary plumbing using galvanized steel pipes, due to water composition or temperature, solid particle deposits, galvanic coupling (with copper, brass or stainless steel for examples) or the presence of roaming currents [7,8,10]. Actually, in anaerobic media, the corrosion of zinc proceeds via two partial reactions [11]. The cathodic reaction corresponds to the reduction of dissolved oxygen and leads to a pH increase, and the anodic reaction involves the dissolution of zinc and leads to weight loss.

* Corresponding author. Tel.: +32 65 37 44 38; fax: +32 65 37 44 36.

E-mail addresses: Fabienne.delaunois@umons.ac.be (F. Delaunois), Francois.tosar@umons.ac.be (F. Tosar), Veronique.vitry@umons.ac.be (V. Vitry).

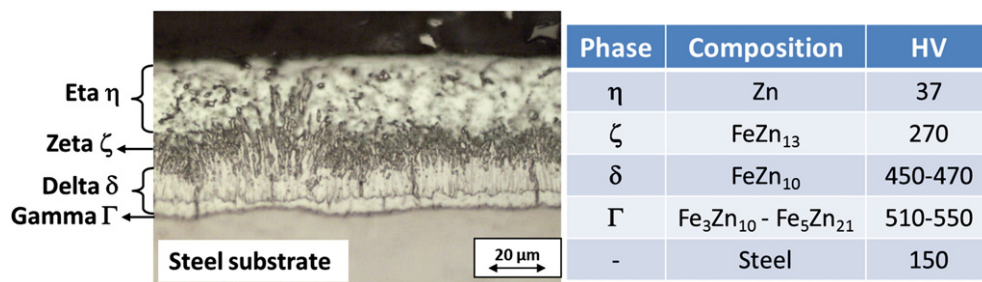


Fig. 1. Optical micrograph of hot-dip galvanized steel (etched with 0.5 vol.% Nital); composition and expected Vickers hardness (HV).

Because corrosion rate of galvanized steel is sometimes too important to be described by common corrosion mechanisms, another type of corrosion has recently been the subject of investigation [12–14]: biocorrosion by sulphate-reducing bacteria (SRB) in oxygen deficient environments, such as plumbing systems, water softeners and water heaters.

Biocorrosion of carbon or stainless steels is a well-known phenomenon occurring in sea medium or in all activities using freshwater sediments and, generally, where bacteria are present and abundant (sea, mud) [15–18]. In the absence of dissolved oxygen as electron acceptor, anaerobic bacteria (like SRB) may reduce sulphate contained in water to sulphite ions, which can be oxidized to hydrogen sulphide H₂S. The electron donor is either H₂ or organic compounds (such as lactate or pyruvate). When H₂ is the electron donor, it is produced by the reduction of hydrogen ion by either zinc (sacrificial anode) or iron which is oxidized to ferrous sulphides [15,19,20]. The organic compounds, on the other hand, are contained and produced by anabolic bacterial cell reactions.

In parallel, the reduction of hydrogen (electron acceptor) is also possible producing adsorbed hydrogen which could be used by bacteria as electron donor. Hydrogen consumption by bacteria still increases corrosion by iron or zinc consumption (electron donor). Moreover, the production of H₂S enhances iron oxidation. This phenomenon could explain corrosion rate in galvanized steel tubes.

Due to the removal of most bacteria from water for drinking, biocorrosion could usually be considered as marginal. Actually, only few studies describe biocorrosion by SRB in potable water means. Seth and Edyvean [21] have noticed frequent occurrences of SRB in drinking water when cast iron pipes are used. They indicated SRB's ability to colonize a new installation quickly, causing an increase of corrosion rate. Ilhan-Sungur and Cotuk [22] highlighted a corrosion rate of 3 μm/y in an abiotic environment against 12 μm/y in a biotic environment for galvanized steel [22]. Moreover, they showed that galvanized steel could be corroded by microorganisms as well as SRB. They assessed that SRB could survive in the mixed species biofilm with very high Zn concentrations. Likewise, a study outlines an increase of corrosion rate from 6 μm per year (μm/y) in abiotic environment to 9.5 μm/y in biotic environment for carbon steel [23]. In some cases, the corrosion rate of galvanized steel can reach 20 μm/y if conditions are favourable to bacterial growth [24].

The object of this paper is to describe microstructures and defects of hot-dip coated galvanized coatings and to present the divergences with optimum structure, as well as to observe various corrosion types in galvanized steel tubes used for sanitary plumbing, and particularly biocorrosion.

2. Materials and methods

2.1. Samples

Various case studies provided us a lot of specimens: (i) new galvanized and new bare steel tubes (16 mm and 22 mm interior diameter galvanized tubes and 16 mm interior diameter steel tubes) and

(ii) 16 mm galvanized and bare steel tubes inserted in parallel in an experimental sanitary mean, as shown in Fig. 2, to simulate a potable water distribution system. Water flow in this simulated sanitary mean was maintained at 3.6 l/min.

Samples were studied in the as-received conditions and after use in our experimental sanitary system. Specimens in the as-received conditions were cut axially with a band saw and some were also cut in cross section. They were then prepared for metallographic examination. The mechanical polishing was processed with a water-free lubricant to avoid further corrosion of the galvanized coating. Thickness of the Zn deposit was measured by optical microscopy, with image analysis software. Etching was carried out with 0.5 vol.% Nital for the Zn coating and with 4 vol.% Nital for bare steel tubes to reveal their microstructure.

2.2. Detection and culture of SRB

The presence of SRB was controlled by a BART test (Biological Activity Reaction Test). The BART method evaluates the rate at which bacteria metabolize the substrate and generate an observable reaction as a result of oxidation, reduction, or enzymatic activity. As results of the SRB-BART™ test, the formation of a black precipitate confirms the presence of SRB.

The presence of SRB in our sanitary water main has been checked by a BART test after 6 months of use in our installation. Tests have been realised on the water seeping out of the galvanized steel tube and of the bare steel tube.

The culture medium was prepared as follows: solution A: MgSO₄ (5 g/l), sodium citrate (12.5 g/l), CaSO₄ (2.5 g/l), NH₄Cl (2.5 g/l), in 400 ml distilled H₂O; solution B: K₂HPO₄ (2.5 g/l) in 200 ml distilled H₂O; and solution C: sodium lactate (8.75 g/l), yeast extract (2.5 g/l) in 400 ml distilled H₂O. The three solutions were mixed after sterilisation in an autoclave at 120 °C during 3 h. Before inoculation, the pH was adjusted to 7.5 with 1 M NaOH.

To favour the development of SRB that could already be present in corroded tubes, tubes were immersed in the culture medium. Reactor temperature was maintained at 37 °C during 2 days. BART tests then were performed on the culture media.

Simultaneously, a culture medium containing SRB was prepared similarly. After sterilisation, a commercial source of SRB (ATCC 7757) was introduced in the culture medium in a reactor under N₂ bubbling (to ensure dissolved oxygen removal and observe effects of bacterial corrosion only) and at 37 °C. Then the tubes were inserted in the reactor

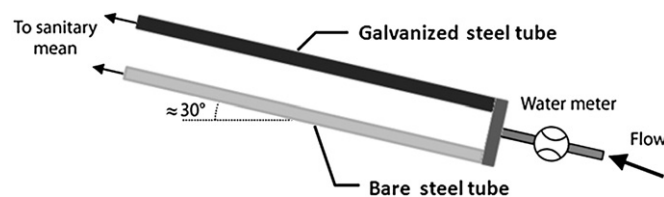


Fig. 2. Bare and galvanized steel tubes installed parallel in laboratory sanitary mean.

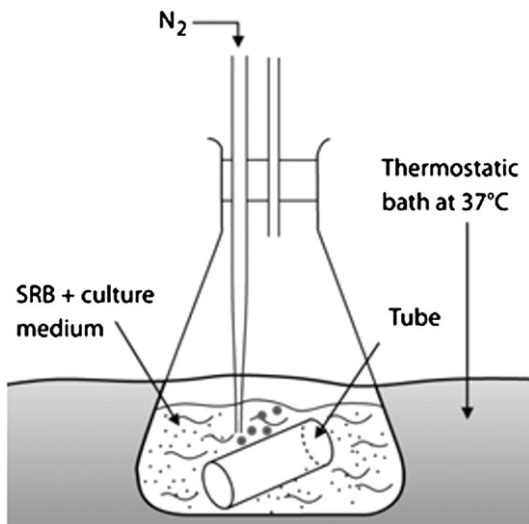


Fig. 3. Reactor for SRB¹
¹ SRB: sulphate-reducing bacteria. culture.

for 10 days (Fig. 3). After this period, tubes were removed and dried, and the corrosion products were characterized.

2.3. Characterization methods

Electrochemical tests were carried out using a Parstat 2273 potentiostat equipped with a frequency response analyzer and a conventional three electrode cell. The cell geometry was designed to expose an area of the sample to the electrolyte with a surface area $A_0 = 3.5 \text{ cm}^2$ for tubes with an interior diameter of 22 mm and of $A_0 = 3.15 \text{ cm}^2$ for tubes with an interior diameter of 16 mm. The experiments were carried out in various electrolytes, at room temperature, with a platinum grid as counter electrode and an Ag/AgCl reference electrode (0.197 V vs. NHE). The various electrolytes used in this research are the following: (i) drinking (tap) water ($K(\text{tapwater}) = 682 \pm 3 \mu\text{S/cm}$), (ii) 0.1 M NaCl aqueous solution: chosen because chloride ion is present in many corrosion situations and in this particular concentration to have a sufficient conductivity for electrochemical measurements [23]

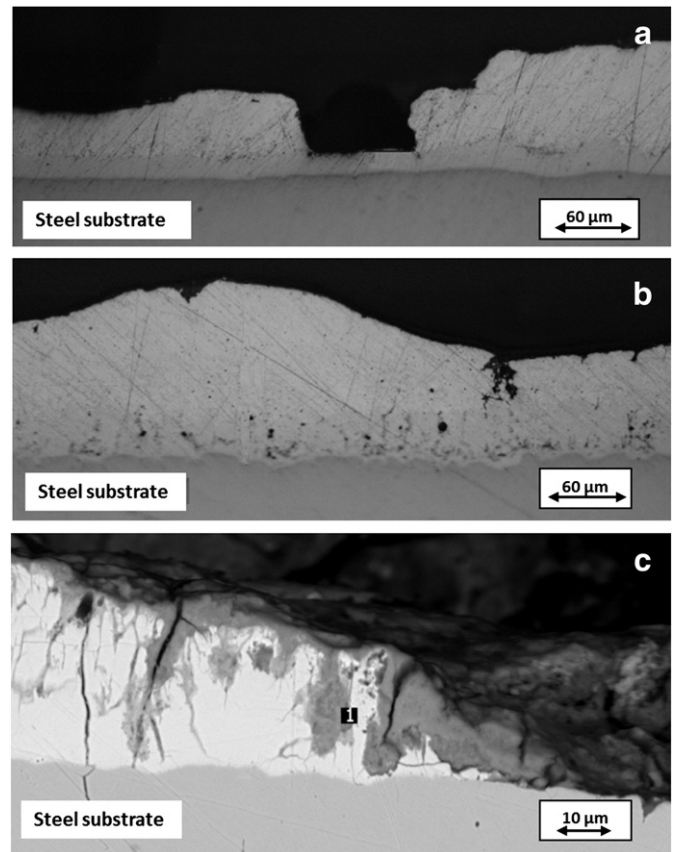


Fig. 5. Optical micrographs of Zn coating defects such as Zn lack (a), overthickness of Zn coating (b); SEM micrograph of Zn coating presenting internal cracks.

($K(0.1 \text{ M NaCl}) = 9.02 \pm 0.5 \text{ mS/cm}$) and (iii) synthetic seawater ($K(\text{artificial seawater}) = 43.4 \pm 0.2 \text{ mS/cm}$); artificial seawater was synthesized with Na^+ , K^+ , Mg^{2+} and Ca^{2+} ions, chloride and sulphate solute concentrations equal to that proposed by Millero [26], NaCl content close to 0.5 M. Before each experiment, a settling time of 15 min was observed to allow stabilization of the open circuit potential (OCP).

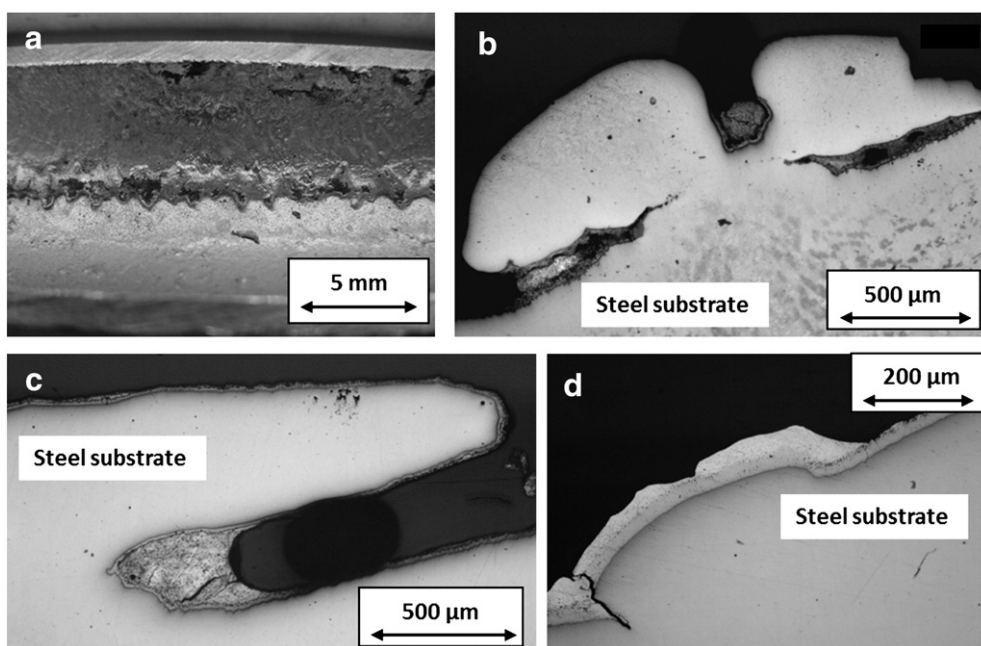


Fig. 4. Optical micrographs of welding defects in large galvanized tubes (a), such as blister (b and c) or internal crack (d).

Table 1

Thickness ($T/\mu\text{m}$) of zinc coatings a 10 cm long section of galvanized tube depending on position along the tube (Distance D/cm) and angular position from welding ($\phi/^\circ$).

D (cm)	ϕ ($^\circ$)	T (μm)					
		0	2	4	6	8	10
0	0	50	46	31	39	37	38
	90	50	56	35	56	47	40
	180	25	26	39	47	37	41
	−90	35	46	42	35	42	56

Numbers in bold are those that follow the european standard.

The electrochemical polarization or Tafel curves were recorded by scanning the potential from -250 to $+250$ mV from the open circuit potential (OCP); sweep rate $v = 10$ mV/min.

The electrochemical impedance spectroscopy (EIS) measurements were carried out at open circuit potential with a sinusoidal signal perturbation of 5 mV, in the frequency range 10^5 to 10^{-2} Hz.

Some samples were observed by SEM (scanning electron microscopy) and EDS (Energy dispersive X-ray spectroscopy) using a Jeol JSM 5900 LV scanning electron microscope.

The corrosion products were investigated by X-ray diffraction, with a Philips X-ray apparatus applying Co $K\alpha$ radiations (1.7902 \AA). SEM and EDS analyses were also used to characterize corrosion products.

The water composition (nitrate, sulphate and chloride ions) were performed with UV-visible spectrometer HACH, using proprietary HACH methods.

3. Results

3.1. Optimum galvanized steel coating microstructure

Fig. 1 shows the microstructure expected of a zinc coating to provide good corrosion protection of the steel substrate in water. As said in

Section 1, the protective outer pure zinc eta layer must represent, in thickness, at least 45% ($25 \mu\text{m}$) of the whole galvanized coating (about $55 \mu\text{m}$).

3.2. Defects observed in galvanized coatings on steel

Tubes in the as-received conditions have been observed by stereomicroscopy and optical microscopy. The bare steel tube presents a classical microstructure with a ferritic matrix and tertiary cementite at the grain boundaries. The steel of galvanized tubes presents a structure with a majority of proeutectoid ferrite and a small amount of perlite. Some defects can be observed on the welding of large galvanized steel tubes, such as blisters or cracking (Fig. 4). Important irregularities of the coating thickness can also be observed: from nothing to about $100 \mu\text{m}$, and sometimes more (Fig. 5(a) and (b)). The European standard EN 10240 imposes a minimum of $55 \mu\text{m}$ of zinc at the interior side of the galvanized steel tube, and $28 \mu\text{m}$ on the welding [10]. Measurements of galvanized coating thickness along a 10 cm long section of tube show that the standard is most of the time not respected (Table 1). Moreover, the average thickness of this sample ($41.5 \pm 8.6 \mu\text{m}$) is less than that required by the European standard. A precise observation (by SEM) of the galvanized coating also shows the presence of internal cracks (Fig. 5(c)).

Fig. 6 shows moreover that, even when the minimum thickness of $55 \mu\text{m}$ is respected, the microstructure of the galvanized coating can be inadequate, with an outer protective pure zinc eta (η) layer too thin to ensure effective protection of the steel substrate against corrosion (Fig. 6(a)). When the coating is very thin (less than $20 \mu\text{m}$) (Fig. 6(b)), its structure is composed of nearly 50% delta (δ) layer–50% zeta (ζ) layer, and the outer protective pure zinc eta (η) layer is missing. In some cases, irregularities of the galvanized coating lead to a too thin pure zinc eta (η) layer, with a zeta (ζ) layer reaching the surface of the coating with a lack of delta (δ) layer in some places, impeding protection of the steel substrate against corrosion (Fig. 6(c)).

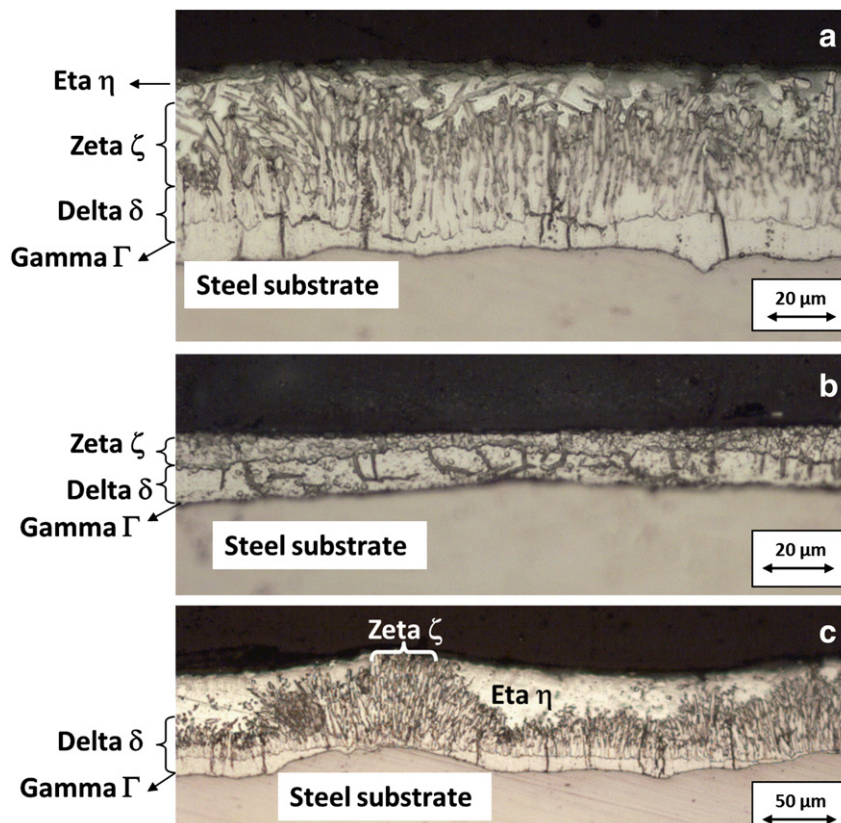


Fig. 6. Optical micrographs of hot-dip galvanized steel defects (etched with 4 vol.% Nital), such as too thin η -layer (a), missing η -layer (b) and irregularities as ζ -layer reaching the surface (c).

3.3. Corrosion behaviour of galvanized steel tubes used in sanitary mean

The corrosion behaviour of galvanized steel tubes with 22 mm interior diameter was studied.

Fig. 7 shows the evolution of the OCP of 2 galvanized steel tubes during 60 min of immersion in various electrolytes: one presents a zinc coating with an adequate microstructure and homogeneous thickness (over 55 μm) and is exempt of defects (named “good galvanized steel tube”; Fig. 7(a)) and one has a galvanized coating of lesser (bad) quality, with the presence of many defects, inadequate microstructure and heterogeneous thickness (named “bad galvanized steel tube”; Fig. 7(b)). As expected [11,23,27], the OCP shifts gradually towards more positive values and thus the behaviour of the system becomes nobler due to the formation of a passive layer on the top of the zinc during the immersion in the electrolyte in the case of good galvanized steel, excepted in 0.1 M NaCl. Actually, in 0.1 M NaCl, the zinc coating is attacked by chloride that degrades the coating protection at the beginning of immersion. After about 40 min of immersion, the OCP becomes nobler with the formation of the corrosion products. In artificial seawater electrolyte, the activity of sodium chloride is weakened by the presence of other ions such as K^+ , Mg^{2+} , Ca^{2+} and SO_4^{2-} . In the case of bad quality galvanized steel tube, during the very first moments of immersion, the OCP shifts to less noble values due to enhancement of the anodic dissolution of the coating. When corrosion products are deposited on the surface, the potential gradually shifts in the noble direction. Moreover, this effect

is of little significance as long as the dissolution of the coating does not expose bare areas of steel substrate [23].

Fig. 8 shows the Tafel plots of the polarization curves from a good quality galvanized steel tube (Fig. 8(a)) and a bad quality galvanized coating (Fig. 8(b)) in various electrolytes. Before starting the measurement, samples are kept in 0.1 M NaCl solution for 15 min, to allow the covering of the coating surface by a very thin layer of zinc oxide [27]. Values of the electrochemical corrosion parameters (corrosion potential E_{corr} (V vs. Ag/AgCl), corrosion current density j_{corr} ($\mu\text{A}/\text{cm}^2$)) are shown in Table 2.

Table 2 shows that, for each electrolyte used, the corrosion potential E_{corr} of the good and bad quality galvanized steel tubes are in the same range if the standard deviation is taken into account. The presence of chloride in important concentration causes a shift in corrosion potential to more negative values compared to drinking water. Moreover, the corrosion current density j_{corr} is higher for the bad quality galvanized coating whatever the electrolyte. For the good quality galvanized steel tube, as expected from the OCP results, the corrosion current density j_{corr} for 0.1 M NaCl electrolyte is higher than that for artificial seawater electrolyte due to the higher activity of the chlorides in 0.1 M NaCl. Fig. 8 shows that, at the beginning of the anodic branch of the Tafel curves, the current sharply increases and there is no passive region. The increasing potential is then responsible for the active dissolution of zinc and dissolution continues until the zinc surface is covered by a layer of corrosion

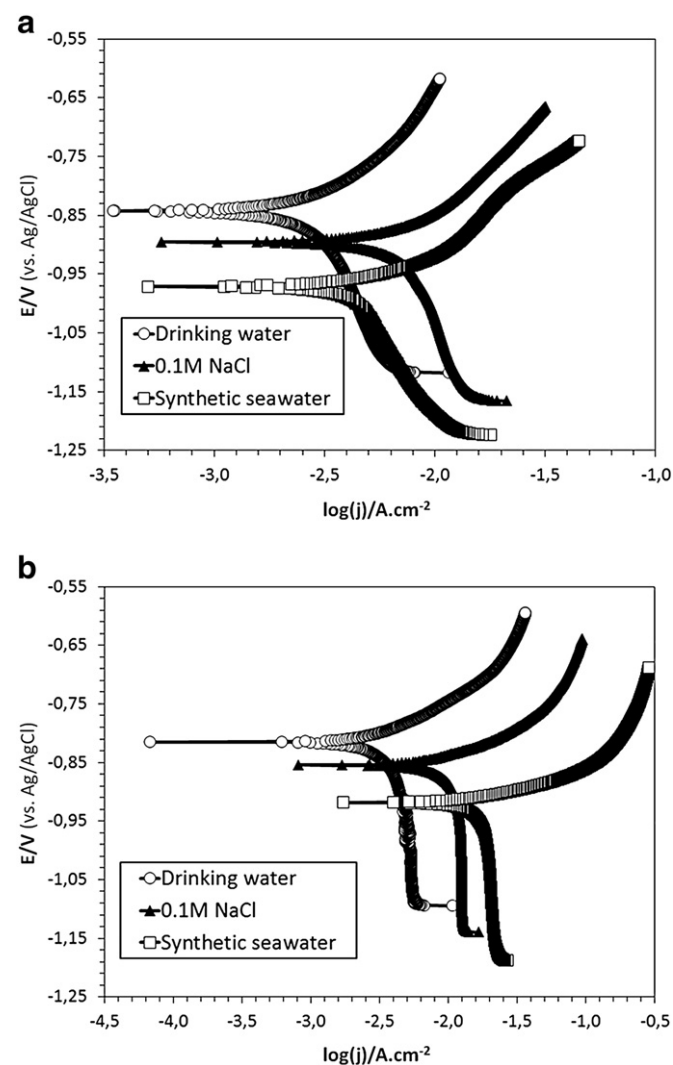
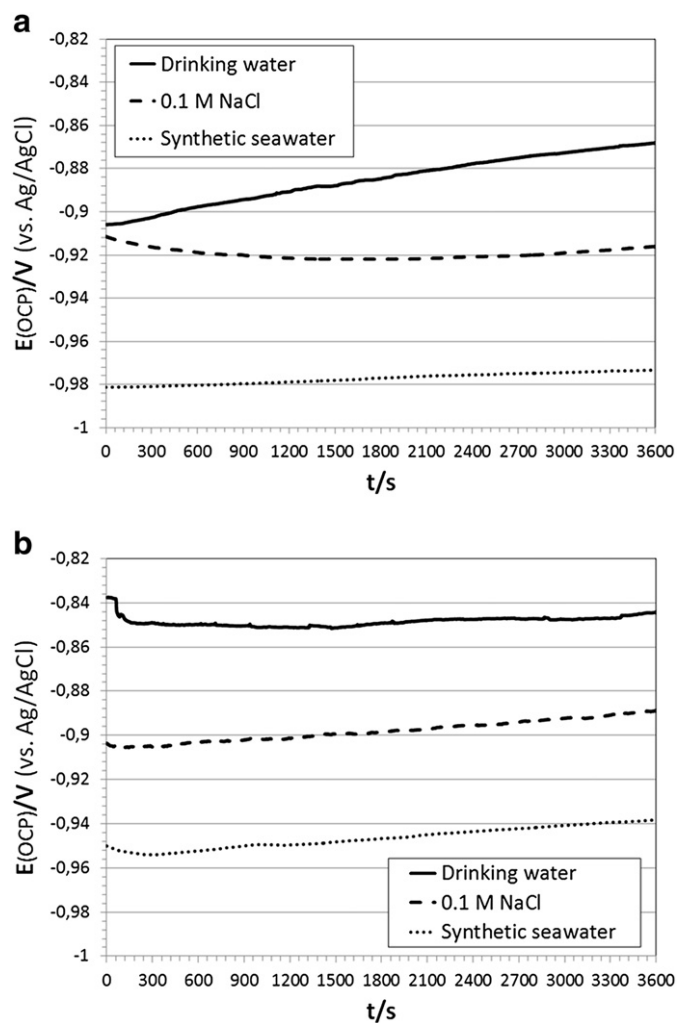


Fig. 7. Open circuit potential E_{OCP} of good quality (a) and bad quality (b) large galvanized steel tube in various electrolytes vs. time of immersion.

Fig. 8. Potentiodynamic polarization curves of a good quality (a) and bad quality (b) large galvanized steel tubes in various electrolytes.

Table 2

Corrosion parameters – potential E_{corr} (V vs. Ag/AgCl) and current density j_{corr} ($\mu\text{A}/\text{cm}^2$) – determined from Tafel plots for a good and a bad galvanized steel tube in various electrolytes. The error is expressed in standard deviation, established from 5 experiments.

	Good galvanized steel tube			Bad galvanized steel tube		
	Drinking water	0.1 M NaCl	Synthetic seawater	Drinking water	0.1 M NaCl	Synthetic seawater
E_{corr} (V vs. Ag/AgCl)	-0.859 ± 0.017	-0.882 ± 0.014	-0.970 ± 0.002	-0.858 ± 0.043	-0.865 ± 0.010	-0.942 ± 0.024
j_{corr} ($\mu\text{A}\cdot\text{cm}^{-2}$)	0.90 ± 0.02	3.84 ± 0.43	2.22 ± 0.00	3.79 ± 1.76	20.04 ± 7.36	41.34 ± 5.31

products, that is not a passive layer but only a pseudo-passive layer [11]. At the end of the anodic curve, the current density does not drop with the increase of potential.

The Nyquist impedance diagrams as a function of immersion time for good galvanized steel tubes, in large size (22 mm interior diameter), in various electrolytes are shown in Figs. 9 and 10.

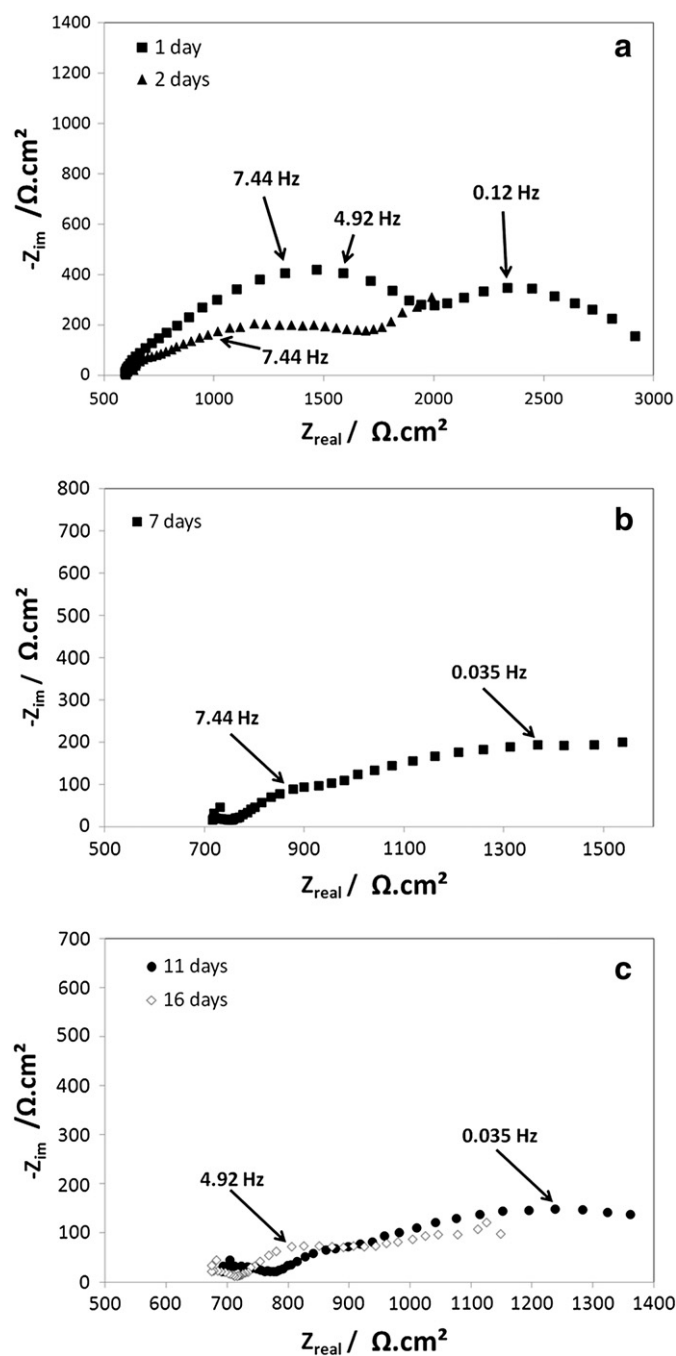


Fig. 9. Nyquist plots of Electrical Impedance Spectroscopy data for 1–2 days (a), 7 days (b) and 11–16 days (c) of immersion in 0.1 M NaCl of a large galvanized steel tube (imaginary part vs. real part of complex impedance).

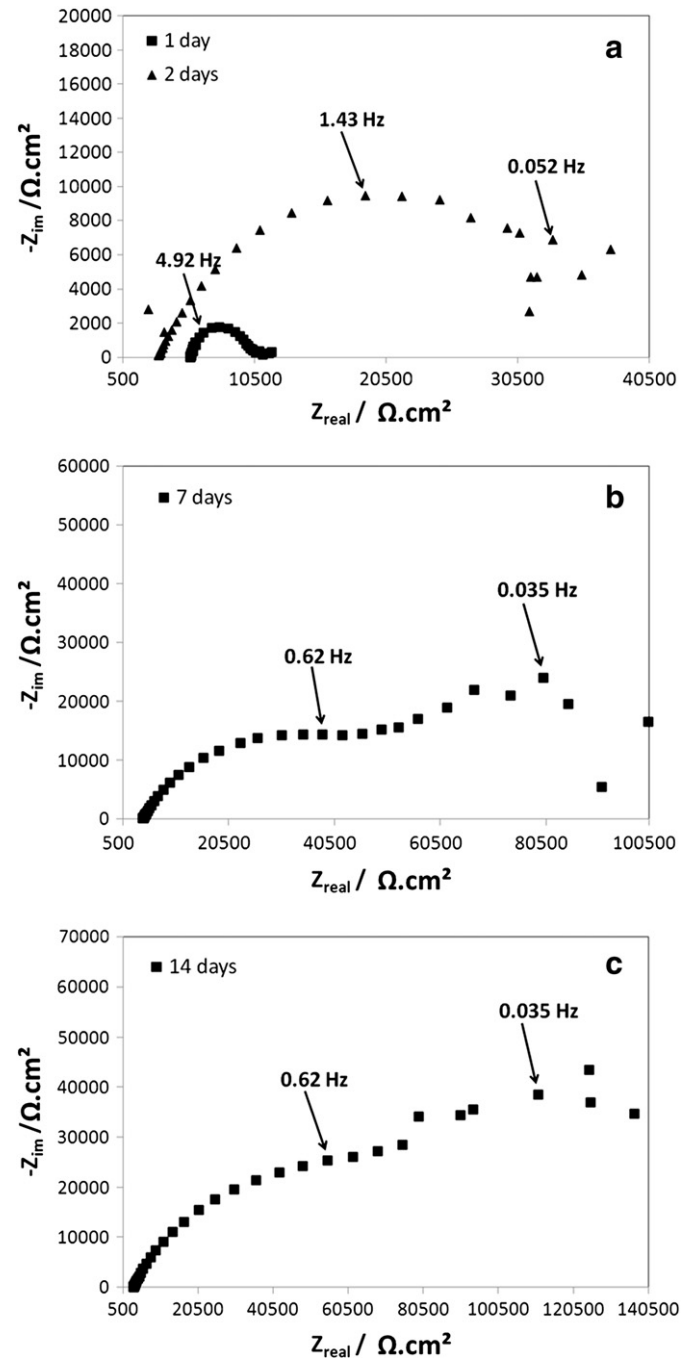


Fig. 10. Nyquist plots of EIS data for 1–2 days (a), 7 days (b) and 14 days (c) of immersion in drinking water of a large galvanized steel tube (imaginary part vs. real part of complex impedance).

In 0.1 M NaCl solution (Fig. 9), we observed an arc (or depressed semicircle) at high and medium frequencies (HF–MF) followed by a second arc at low frequency (LF) (Fig. 9(a)). As the immersion time increases, the LF arc or tail becomes more important and the high frequency–medium frequency (HF–MF) arc is seriously depressed. Nyquist impedance curves obtained in drinking water (Fig. 10) can be interpreted similarly. Moreover, the solution resistance is higher in drinking water than that in 0.1 M NaCl solution and the diffusion process at LF is more noticeable.

Figs. 11 and 12 show the Bode modulus (a) and Bode phase (b) plots of EIS results for good quality galvanized steel tube (22 mm interior diameter) in various electrolytes as a function of immersion time.

In 0.1 M NaCl solution (Fig. 11), the low frequency impedance modulus value (Fig. 11(a)) that reaches $3.10^3 \Omega \cdot \text{cm}^2$ after one day of immersion, decreases slowly with immersion time to about $10^3 \Omega \cdot \text{cm}^2$, due to chloride attack of the coating and to the dissolution of zinc. This shows a nearly resistive behaviour of the coating. At low frequencies, the phase angle is less than 10° (Fig. 11(b)). During the first days of immersion, two time constants are detected at low and medium frequencies due to electrochemical activity. The low frequency time constant is attributed to corrosion processes and its shift to lower frequency with immersion time is due to the slowdown of the process related to the diffusion through corrosion products. The appearance of a third time constant at low frequencies after long periods of immersion points out the degradation of the coating. The medium frequency time constant generally relates to the coating. The increase of the phase angle in the low frequency range after 2 days of immersion accounts for corrosion

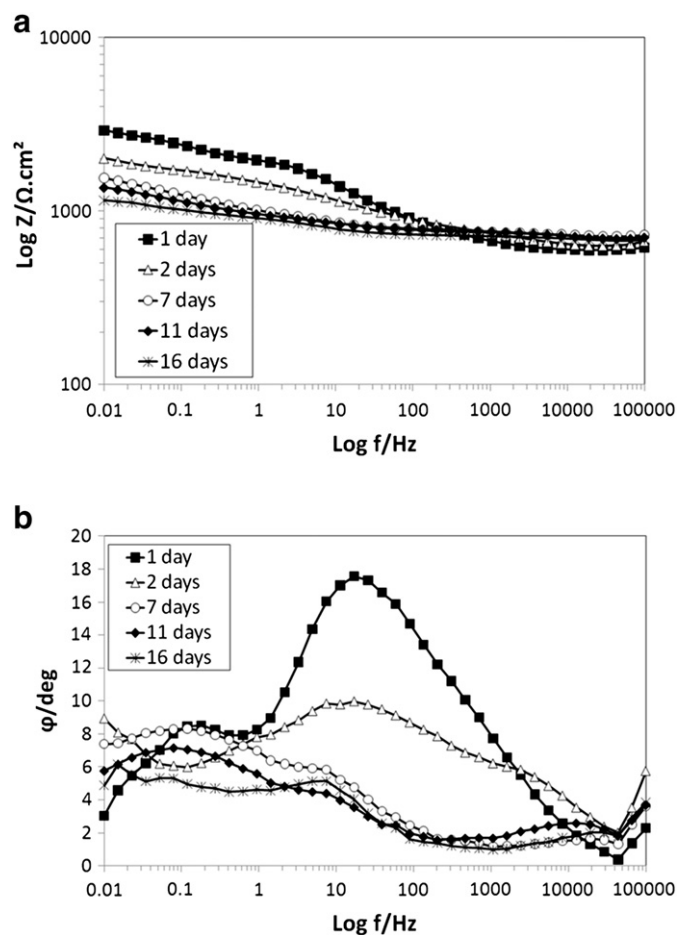


Fig. 11. Bode plot of EIS data for 1–16 days of immersion in 0.1 M NaCl of a large galvanized steel tube (Bode modulus vs. frequency (a) and Bode phase vs. frequency (b)).

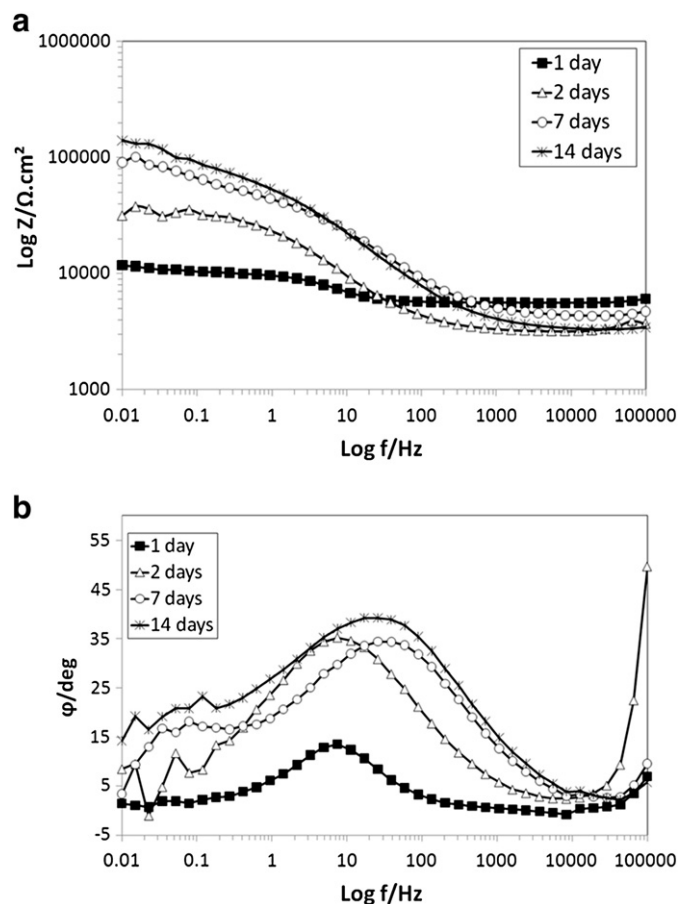


Fig. 12. Bode plot of EIS data for 1–14 days of immersion in drinking water of a large galvanized steel tube (Bode modulus vs. frequency (a) and Bode phase vs. frequency (b)).

initiation. Moreover, it is difficult to fit the EIS spectra with classical equivalent circuits because of corrosion products.

In drinking water (Fig. 12), the observed phenomena are different. The low frequency impedance modulus increases with immersion time from about $10^4 \Omega \cdot \text{cm}^2$ after one day of immersion to reach more than $10^5 \Omega \cdot \text{cm}^2$ after 14 days (Fig. 12(a)). This is due to the formation of a protective zinc hydroxide layer on the surface of the coating. In the Bode phase diagram (Fig. 12(b)), after one day of immersion, we observe only one time constant at medium frequencies related to the coating. At low frequencies, the phase angle that is close to zero degree during the first days of immersion increases to 15° after 14 days of immersion. After 7 days of immersion, two time constants are detected at low and medium frequencies due to corrosion processes.

3.4. Analyses of corrosion products of galvanized steel tubes in sanitary mean

After 6 months of use in the sanitary system installed in our laboratory, samples of the galvanized and of the bare steel tube have been isolated and prepared for SEM and EDS analyses. The bare steel tube presents a strong (as expected) internal generalized corrosion (Fig. 13(a)). The measurement of the tube thickness shows a consumption of $10 \mu\text{m}$, and thus a corrosion rate of $20 \mu\text{m}/\text{y}$. The galvanized steel tube also presents a corrosion film and the dissolution of the η phase of the zinc coating (Fig. 13(b)).

EDS analysis of tube surfaces (Table 3) show the oxidation of iron or zinc, as expected, and different elements coming from water (Ca, Si, P, ...). Sulphur and chlorine are also detected in the two tubes, with bigger amounts of both elements in the galvanized one.

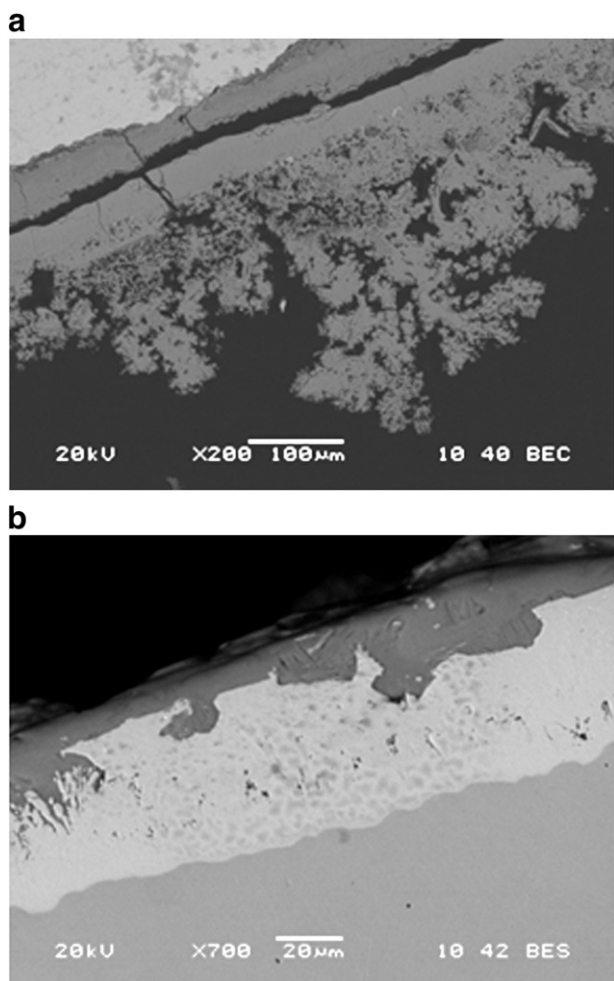


Fig. 13. SEM micrographs of bare (a) and galvanized (b) steel tubes after 6 months of use in sanitary system in laboratory.

3.5. Water composition of sanitary mean

After 1 month of use in the sanitary system installed in our laboratory, a sample of water was taken from the output of each tube and from the input of the installation and analysed for nitrate, sulphate and chloride composition. Results are provided in Table 4.

Those results show a decrease of sulphate and an increase of chloride ion concentrations in the output of sanitary mean. Nitrate concentration stays constant.

3.6. Biocorrosion

After 6 months of use in the sanitary system installed in our laboratory, a detection test for SRB was performed on the water seeping out the tubes and on corrosion products. To increase the detection level of the BART test, microbial culture was carried out for 2 days on a sample of each tube in sterilised culture medium. Then, a BART test was

Table 4

Water composition analyses from output of galvanized and bare steel tubes and from input (index) of sanitary mean (mg/l). The error is expressed in standard error of measurement.

	Nitrate (mg/l)	Sulphate (mg/l)	Chloride (mg/100 ml)
Index	13.2 ± 0.2	75.0 ± 0.2	4.8 ± 0.4
Galvanized steel tubes	13.4 ± 0.2	67.3 ± 0.2	6.6 ± 0.4
Bare steel tubes	13.0 ± 0.2	69.5 ± 0.2	6.4 ± 0.4

performed on each culture medium during 10 days. The results illustrated in Fig. 14 show the positive detection of SRB in the culture medium used for the bare tube and the negative detection for the galvanized steel tube. These results also prove the presence of SRB in potable water in the area our lab is situated in. The negative result for the galvanized steel tube and sanitary water can be attributed to a lower level of SRB, possibly under the level of detection of a BART test. The negative result does not support the conclusion that SRB is absent of sanitary water, but that they are present in too small quantity for BART test.

From the start of laboratory mean use, samples of galvanized and bare tube were collected, after 2, 3 and 6 months of use, for SRB detection (BART test). However BART tests were always negative, perhaps due to the low SRB concentration. Thus, a sterilised culture medium was used to increase SRB population before tests. Time of culture and time before BART test reaction are shown in Table 5.

The bare steel tube was the first to react with BART test all along the test time. Bacteria community is thus more important in bare steel tube than in galvanized steel one. Moreover, if reaction times (at 2 and 6 months) are compared for each tube, it is noted that it strongly decreased although the culture time was also shortened.

3.7. Influence of SRB bacteria on galvanized and on bare steel tubes

In order to highlight SRB influence, a sample of new galvanized and new bare steel tubes has been inserted in a culture medium inoculated with a commercial source of SRB. After 5 days of immersion, the formation of a black precipitate in the reactors and H₂S release (high added smell) were observed in two samples. The experiment was performed for 10 days.

SEM observation of the internal surface of the bare steel tube (Fig. 15(a)) shows generalized corrosion with some pitting. The galvanized steel tube (Fig. 15(b)) presents an important corrosion penetration: 10 µm of the zinc coating is affected and some micro-cracks are observed. This corrosion differs from the pitting corrosion observed in other works [25].

EDS analyses of the internal surface of galvanized steel tube shows oxidation of the zinc coating. The presence of sulphur and chlorine (Table 3) is also widely detected.

4. Discussion

Standard corrosion phenomena do not suffice to explain all the cases of pipe failures. Therefore, new metallographic investigations on galvanized steel tubes and on the zinc coating itself were performed. Results showed the frequent occurrence of defects in the welding, such as blisters or cracks, and also in the coating. Cracks have been identified

Table 3

EDS^a analysis of the corroded surface of galvanized and bare steel tubes after 6 months of use in sanitary system and after 10 days in a medium containing SRB (in atomic %/at.%).

Element (at.%)		Fe	O	Si	S	Cl	Ca	Pb	Zn	P
Bare steel tube	After 6 months in use	38.67	60.01	0.33	0.26	0.16	0.35	–	–	–
Galvanized steel tube	After 6 months in use	1.88	52.51	0.81	1.82	1.46	0.22	0.95	39.63	0.72
Bare steel tube	After 10 days in SRB medium	33.37	60.06		0.73	0.44				
Galvanized steel tube	After 10 days in SRB medium	43.96	52.48		2.11	1.46				

The numbers in bold are those that interest us in the study.

^a EDS: Energy Dispersive X-ray Spectrometry.

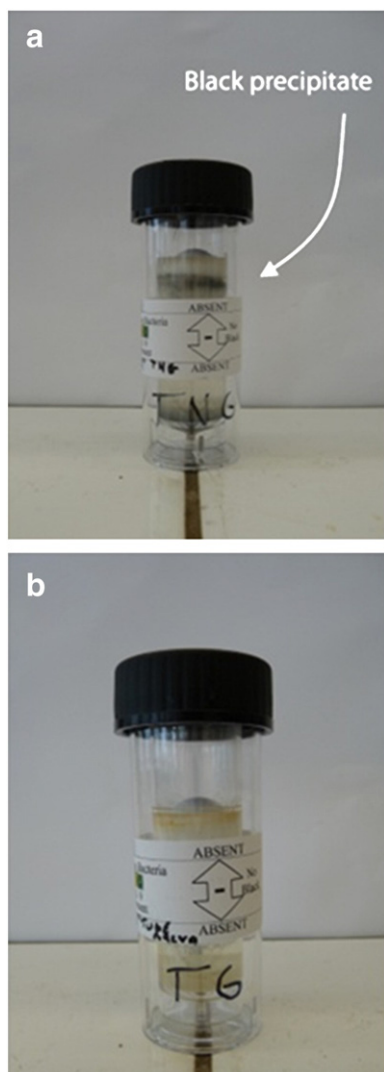


Fig. 14. BART²
² BART: Biological Activity Reaction Test. test for water seeping out the bare (a) and galvanized (b) steel tubes.

in the coating, near the substrate, and sometimes even inside the substrate (Fig. 4). In Table 1, we have observed important irregularities of the coating thickness, with coatings not following the European standard (which imposes a minimum thickness of 55 μm on the inside of galvanized steel tubes, and 28 μm on the welding). Moreover, the metallographic structure of the zinc coating itself does not correspond to expectations: the outer protective pure zinc eta (η) layer is sometimes too thin to offer effective protection against corrosion to the steel substrate and can even be absent in some cases (Fig. 5).

Table 5
 Time of SRB^a culture and time before BART^b test reaction depending on sampling time.

	Sampling time	Culture time (d)	Reaction time (d)
Bare steel tube	After 2 months in use	29	41
	After 3 months in use	39	32
	After 6 months in use	19	4
Galvanized steel tube	After 2 months in use	29	No reaction
	After 3 months in use	39	45
	After 6 months in use	19	No reaction

^a SRB: sulphate-reducing bacteria.
^b BART: Biological Activity Reaction Test.

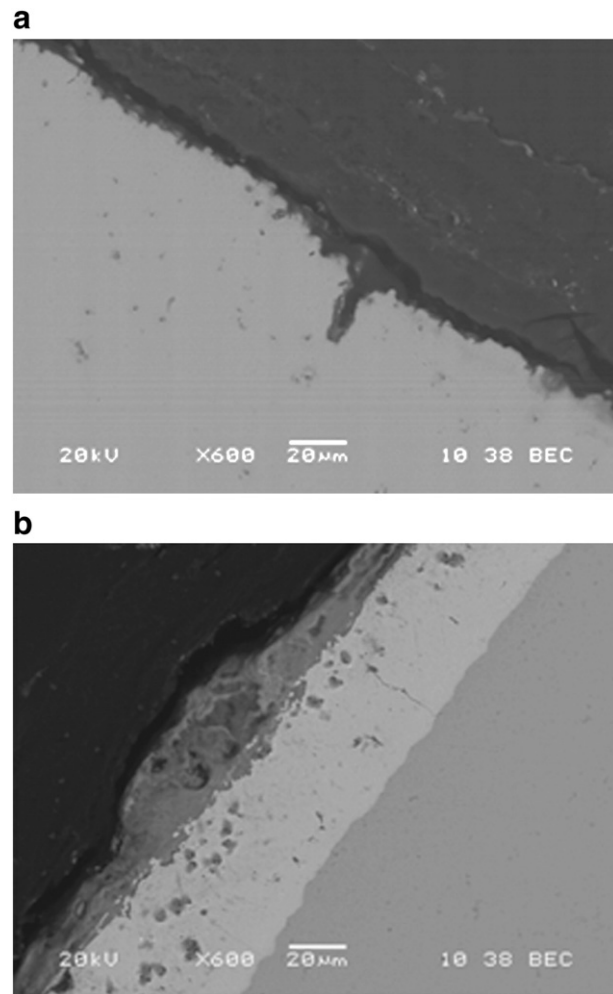


Fig. 15. SEM micrographs of bare (a) and galvanized (b) steel tubes after 10 days in culture medium.

All these observations allow us to say that many pipe failures in potable water distribution system are notably due to the bad quality of the galvanized coating and to defects in the welding.

Electrochemical studies of corrosion provide information about corrosion behaviour of galvanized steel tubes in water. Firstly, after immersion in drinking water and in synthetic seawater, OCP (Fig. 7) of the good galvanized steel tubes becomes more positive due to the formation of a passive layer of zinc oxides. Bad galvanized steel tubes have more trouble to form an effective passive layer in all the electrolytes that were studied. Secondly, Tafel curves (Fig. 8) indicate that the corrosion process is totally or partially dependent on diffusion through the layer of corrosion products. Table 2 shows that the rate limiting step is the mass transfer of corrosion reagents due to the zinc deposit acting as a barrier coating, controlling the reaction of dissolved oxygen [11,23,27]. Thus, corrosion by neutral aerated water is not promoted but this oxygen gradient is favourable for anaerobic bacteria which find a friendly environment. Finally, Nyquist plots (Figs. 9 and 10) and EIS analysis (Figs. 11 and 12) confirm this observation. Actually, the LF arc or tail indicates a diffusion process through a finite thickness layer (the corrosion products), related mainly with the reduction of dissolved oxygen, due to the absorbed species that contribute to the formation of the corrosion layer. The HF–MF arc is attributed to faradic charge transfer, associated with the effect of ionic double layer capacitance. This complex mass transport mechanism is due to the system formed by corrosion medium/corrosion products/metal [11,23]. Diagrams at LF give information on the barrier effect of the coating. The appearance of diffusion tails at LF can be linked to the accumulation of corrosion

products [28]. This latter observation is also important for biocorrosion. Actually, this may be explained by the formation, due to corrosion, of a porous interface favourable for the development of bacteria on bare steel tubes. Further investigations have identified another reason for water leakage: SRB activity. Fig. 13 provides an estimation of corrosion rate, about 20 $\mu\text{m}/\text{y}$. An explanation of this high corrosion rate is either an extremely abiotic aggressive water (extreme pH or presence of Cl^-) or biotic water (containing SRB). Indeed, corrosion rate of galvanized steel in abiotic freshwater is always less important [22].

EDS analysis of corrosion by-products, provided in Table 3, have highlighted the presence of chlorine and sulphur in by-products. The presence of chlorine can be associated to the chemical composition of potable water but sulphur cannot. Actually, elemental sulphur can find its origin in the reduction of the sulphate contained in water by SRB. Moreover, water composition analyses, provided in Table 4, show a decrease of sulphate, which would justify the sulphur presence in corrosion products. It may come from sulphate consumption due to SRB growth. The chloride ion increase may be assigned to consumption of (bound or free) chlorine by SRB as electron acceptor (instead of sulphate) [29]. Over the 6 months of use, BART test always showed the presence of SRB in bare steel tubes and sometimes in galvanized steel (depending on culture time). Results included in Table 5 confirm the SRB ability to colonize quickly a new installation with an increase of corrosion rate, and in particular the bare steel tube, which is more favourable to corrosion development. Although the galvanized steel tube seemed more resistant, SRB were also present, leading to a raise of the corrosion rate. This testing campaign shows that culture medium use may be important for SRB detection. Actually, without the culture phase, sanitary water and galvanized steel tube would be “free” of SRB. With the use of culture medium, the presence of SRB can be demonstrated and the link between high corrosion rate and SRB is established.

5. Conclusions

A multiple approach study was used to investigate the corrosion of galvanized steel tubes in drinking water distribution systems. Specifically, surface, thickness and microstructure analysis, various corrosion phenomena and biocorrosion, as well as electrochemical studies are reported. The following conclusions are drawn:

- The quality of galvanized steel tubes is generally not good, with the presence of many defects, and the galvanized coating does not reach specifications of the European standard to be used in plumbing: thickness of the coating (expected to be higher than 55 μm) is frequently too low, and coating microstructure is often inadequate.
- Electrochemical and EIS analysis in various electrolytes (drinking water, 0.1 M NaCl, synthetic seawater) show the role of the zinc coating in cathodic steel protection: the coating acts as a barrier protection with the presence of a diffusion process, related mainly to the reduction of dissolved oxygen. Moreover, the limiting step being oxygen diffusion, an oxygen gradient occurred and anaerobic area appears.
- As a consequence of culture medium use, positive detection of SRB in galvanized and bare steel tubes from a sanitary mean proves the presence of SRB activity in potable water.
- Sulphate metabolism by SRB generates oxidizing agents (such as H_2S) which can react strongly with zinc coating and iron, leading to a quick and important corrosion of the galvanized and the bare steel tubes, underlined by sulphur apparition in corrosion by-products (EDS analyses).

In future work, the focus will be brought on the behaviour of experimental water means after various exposition times, to get more information about the kinetics of biocorrosion (by SRB) in water means. Reflexions about the needs for better quality of HDG steel tubes will also be carried out.

Acknowledgments

The authors thank Prof. Olivier and Mrs. Druart from the Materials Science Dept at UMONS for their help with the analysis of EIS results, and Dr. Gérard Quoirin, Miss Adeline Sens and Mr. Guillaume Richeux for their participation to the study.

References

- [1] AWWARF, Internal Corrosion of Water Distribution Systems, AWWARF-DVGW-TZW Cooperative Research Report, Denver, CO, 1996. (586 pp.).
- [2] A.R. Marder, A review of the metallurgy of zinc coated steel, *Prog. Mater. Sci.* 45 (3) (2000) 191–271.
- [3] C. Volk, E. Dundore, J. Schiermann, M. Lechevallier, Practical evaluation of iron corrosion control in a drinking water distribution system, *Water Res.* 34 (6) (2000) 1967–1974.
- [4] D. Quantin, Galvanization à chaud: Principes, Techniques de l'Ingénieur, M 1 530, 2004. 1–7.
- [5] Hot-Dip Galvanizing for Corrosion Protection: A Specifiers Guide, American Galvanizers Association, 2006. 1–21.
- [6] P.G. Rahrig, Galvanized steel in water and wastewater infrastructure, *Mater. Perform.* 42 (7) (2003) 58–60.
- [7] F. Delaunois, G. Guerlemont, Study of the Corrosion of Galvanized Steel Tubes Used in Water Distribution Systems, *Chimie Nouvelle*, 2008. 15–20.
- [8] Présence de rouille dans l'eau de distribution, Guide pratique des défauts de construction, Installations-plomberie sanitaire et industrielle, CSTC, 1997. 190–191.
- [9] A. Koukalova, K. Kreislova, P. Strzyz, The evaluation of corrosion damage of galvanized tubes for hot water distribution, 2nd International Conference Corrosion and Material Protection, 19–22 April 2010, Prague, Czech Republic, EFC Event No. 322, 2010, ISBN 978-80-90393-6-3.
- [10] C. Callandit, Corrosion des tuyauteries sanitaires en acier galvanisé, CSTC-Contact, 14, 2007, pp. 7–8.
- [11] M. Mouanga, P. Berçot, Comparison of corrosion behaviour of zinc in NaCl and in NaOH solutions; part II: electrochemical analyses, *Corros. Sci.* 52 (12) (2010) 3993–4000.
- [12] I.S. Pogrebova, I.A. Kozlova, L.M. Purish, S.E. Gerasika, O.H. Tuovinen, Mechanism of inhibition of corrosion of steel in the presence of sulfate-reducing bacteria, *Mater. Sci.* 37 (5) (2001) 754–761.
- [13] D. Cetin, M.L. Aksu, Corrosion behavior of low-alloy steel in the presence of *Desulfotomaculum* sp., *Corros. Sci.* 51 (8) (2009) 1584–1588.
- [14] L.K. Herrera, H.A. Videla, Role of iron-reducing bacteria in corrosion and protection of carbon steel, *Int. J. Biodeterior. Biodegrad.* 63 (7) (2009) 891–895.
- [15] W. Lee, Z. Lewandowski, P.H. Nielsen, et al., Role of sulphate-reducing bacteria in corrosion of mild steel: a review, *Biofouling* 8 (1995) 165–194.
- [16] F. Sarioglu, R. Javaherdashti, N. Aksoz, Corrosion of a drilling pipe steel in an environment containing sulphate-reducing bacterial, *International J. Press. Vessel. Pip.* 73 (2) (1997) 127–131.
- [17] R. Javaherdashti, A review of some characteristics of MIC caused by sulfate-reducing bacteria: past, present and future, *Anti-Corr. Methods Mater.* 46 (3) (1999) 173–180.
- [18] F.A. Lopes, P. Morin, R. Oliveira, L.F. Melo, Interaction of *Desulfovibrio desulfuricans* biofilms with stainless steel surface and its impact on bacterial metabolism, *J. Appl. Microbiol.* 101 (5) (2006) 1087–1095.
- [19] R. Marshal, Involvement of sulfidogenic bacteria in iron corrosion, *Oil Gas Sci. Technol. Rev. IFP* 54 (5) (1999) 649–659.
- [20] O.J. Hao, J.M. Chen, L. Huang, et al., Sulfate-reducing bacteria, *Crit. Rev. Environ. Sci. Technol.* 26 (1) (1996) 155–187.
- [21] A.D. Seth, R.G.J. Edyvean, The function of sulfate-reducing bacteria in corrosion of potable water mains, *Int. J. Biodeterior. Biodegrad.* 58 (2006) 108–111.
- [22] E. Ilhan-Sungur, A. Çotuk, Microbial corrosion of galvanized steel in a simulated recirculating cooling tower system, *Corros. Sci.* 52 (1) (2010) 161–171.
- [23] L. Carpen, P. Rajala, M. Vepsäläinen, M. Bomberg, Corrosion behaviour and biofilm formation on carbon steel and stainless steel in simulated repository environment, *Proceeding Eurocorr*, 2013, p. 1589.
- [24] E. Ilhan-Sungur, N. Cansever, A. Çotuk, Microbial corrosion of galvanized steel by a freshwater strain of sulphate reducing bacteria (*Desulfovibrio* sp.), *Corros. Sci.* 49 (3) (2007) 1097–1109.
- [25] V. Barranco, S. Feliu Jr., S. Feliu, EIS study of the corrosion behaviour of zinc-based coatings on steel in quiescent 3% NaCl solution. Part 1: directly exposed coatings, *Corros. Sci.* 46 (9) (2004) 2203–2220.
- [26] F.J. Millero, 6.01 physicochemical controls on seawater, in: Heinrich D. Holland, Karl K. Turekian (Eds.), *Treatise on geochemistry, The Oceans and Marine Geochemistry*, 6, Elsevier Ltd., UK, 2003, pp. 1–21.
- [27] A.P. Yadav, A. Nishikata, T. Tsuru, Electrochemical impedance study on galvanized steel corrosion under cyclic wet-dry conditions—influence of time of wetness, *Corros. Sci.* 46 (1) (2004) 169–181.
- [28] S.C. Chung, J.R. Cheng, S.D. Chiou, H.C. Shih, EIS behavior of anodized zinc in chloride environments, *Corros. Sci.* 42 (7) (2000) 1249–1268.
- [29] M. Madigan, J. Martinko, *Biologie des micro-organismes*, Brock, Paris, 2007. 583 (668–669).